

# Elimination of Harmonics in a Multilevel Converter With Nonequal DC Sources

Leon M. Tolbert, *Senior Member, IEEE*, John N. Chiasson, *Senior Member, IEEE*, Zhong Du, *Student Member, IEEE*, and Keith J. McKenzie, *Student Member, IEEE*

**Abstract**—Eliminating harmonics in a multilevel converter in which the separate dc sources vary is considered. That is, given a desired fundamental output voltage, the problem is to find the switching times (angles) that produce the fundamental while not generating specifically chosen harmonics. Assuming that the separate dc sources can be measured, a procedure is given to find all sets of switching angles for which the fundamental is produced while lower order harmonics are eliminated. This is done by first converting the *transcendental* equations that specify the elimination of the harmonics into an equivalent set of *polynomial* equations. Then, using the mathematical theory of resultants, all solutions to this equivalent problem can be found. Experimental results are presented to validate the theory.

**Index Terms**—Converter, harmonic elimination, multilevel inverter, resultant theory.

## I. INTRODUCTION

A KEY ISSUE in designing an effective multilevel inverter is to ensure that the total harmonic distortion (THD) in the voltage output waveform is small enough. To do so requires both an (mathematical) algorithm to determine when the switching should be done so as to not produce harmonics and a fast real-time computing system to implement the strategy. Work was reported in [1] and [2] that presented a method to compute the switching angles for the H-bridges in a cascaded converter using the mathematical theory of resultants. In that work, a complete solution was presented for computing all possible switching angles that achieved the requisite fundamental voltage and eliminated lower order harmonics. However, it was assumed that the dc sources were all equal, which will probably not be the case in applications even if the sources are nominally equal.

Here, it is shown how the method in [2] can be extended for the nonequal or varying dc source case. Specifically, eliminating harmonics in a multilevel converter in which the separate dc sources do not have equal voltage levels is considered. That is, given a

desired fundamental output voltage, the problem is to find the switching times (angles) that produce the fundamental while not generating specifically chosen harmonics. This technique differs from that in [3] where the dc level of the sources were controlled to a particular value. In this paper, the lower order harmonics are eliminated making use of whatever value the dc-link voltages are for the H-bridges. Related work includes [4] in which the method in [2] is combined with a single harmonic elimination technique while in [5] a genetic algorithm is used.

Assuming that the separate dc sources can be measured, a procedure is given to find all sets of switching angles for which the fundamental is produced while the fifth and seventh are eliminated. This is done by first converting the *transcendental* equations that specify the elimination of the harmonics into an equivalent set of *polynomial* equations. Then, using the mathematical theory of resultants, all solutions to this equivalent problem can be found. In contrast to numerical techniques (e.g., see [6] and [7]), this method guarantees that all solutions will be found and is a method that can compute the solutions fast enough for online updates (needed as the voltage levels of the dc sources change). Experimental results are presented to validate the theory.

The interest here is a cascade multilevel inverter switching at the fundamental frequency with nonequal dc sources. However, many interesting pulsewidth-modulation (PWM) techniques have been proposed for controlling these inverters, for example, [7]–[9] where in [9] harmonic elimination was studied by phase shifting the carrier frequency.

## II. CASCADED H-BRIDGES

The cascade multilevel inverter consists of a series of H-bridge (single-phase full-bridge) inverter units. As previously mentioned, the general function of this multilevel inverter is to synthesize a desired voltage from several separate dc sources (SDCSs), which may be obtained from batteries, fuel cells, solar cells, and ultracapacitors. Fig. 1 shows a single-phase structure of a cascade inverter with SDCSs [10]. Each SDCS is connected to a single-phase full-bridge inverter. Each inverter level can generate three different voltage outputs,  $+V_{dc}$ , 0, and  $-V_{dc}$  by connecting the dc source to the ac output side by different combinations of the four switches,  $S_1$ ,  $S_2$ ,  $S_3$ , and  $S_4$ . The ac output of each level's full-bridge inverter is connected in series such that the synthesized voltage waveform is the sum of all of the individual inverter outputs. The number of output phase voltage levels in a cascade multilevel inverter is then  $2s + 1$ , where  $s$  is the number of dc sources. An example phase voltage waveform for an 11-level cascaded multilevel inverter with five SDCSs ( $s = 5$ ) and five full

Paper IPCSD-04-072, presented at the 2003 IEEE Applied Power Electronics Conference and Exposition, Miami Beach, FL, February 9–13, and approved for publication in the IEEE TRANSACTIONS ON INDUSTRY APPLICATIONS by the Industrial Power Converter Committee of the IEEE Industry Applications Society. Manuscript submitted for review February 1, 2003 and released for publication October 25, 2004. This work was supported in part by the National Science Foundation under Contract NSF ECS-0093884, and in part by Oak Ridge National Laboratory under UT/Battelle Contract 4000007596.

L. M. Tolbert, J. N. Chiasson, and Z. Du are with the Department of Electrical and Computer Engineering, The University of Tennessee, Knoxville, TN 37996-2100 USA (e-mail: tolbert@utk.edu; chiasson@utk.edu; zdu1@utk.edu).

K. J. McKenzie is with The Bradley Department of Electrical and Computer Engineering, Virginia Polytechnic Institute and State University, Blacksburg, VA 24061-0111 USA.

Digital Object Identifier 10.1109/TIA.2004.841162

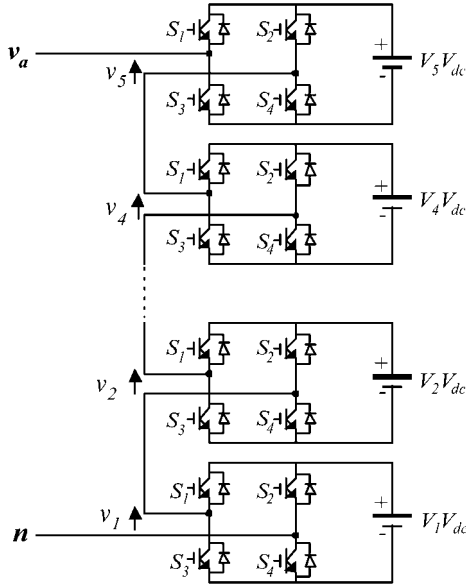


Fig. 1. Single-phase structure of a multilevel cascaded H-bridges inverter.

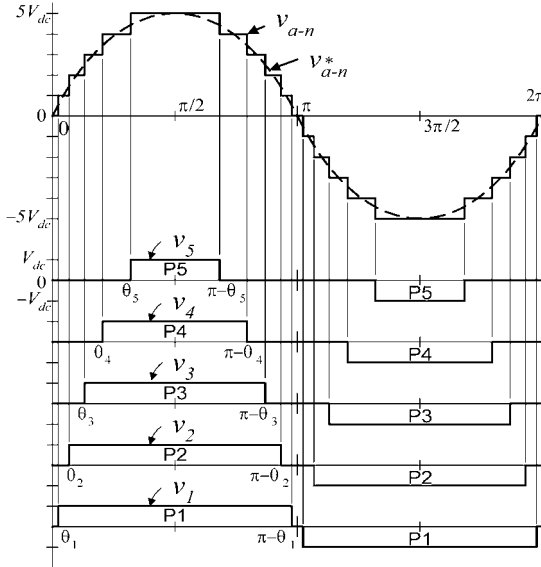


Fig. 2. Output waveform of an 11-level cascade multilevel inverter.

bridges is shown in Fig. 2. The output phase voltage is given by  $v_{an} = v_1 + v_2 + v_3 + v_4 + v_5$ .

With enough levels and an *appropriate* switching algorithm, the multilevel inverter results in an output voltage that is almost sinusoidal. For the 11-level example shown in Fig. 2, the waveform has less than 5% THD with each of the active devices switching only at the fundamental frequency.

### III. SWITCHING ALGORITHM FOR THE MULTILEVEL CONVERTER

The Fourier series expansion of the (stepped) output voltage waveform of the multilevel inverter with *nonequal* dc sources is

$$V(\omega t) = \sum_{n=1,3,5,\dots}^{\infty} \frac{4V_{dc}}{n\pi} (V_1 \cos(n\theta_1) + \dots + V_s \cos(n\theta_s)) \sin(n\omega t) \quad (1)$$

where  $s$  is the number of dc sources, and the product  $V_i V_{dc}$  is the value of the  $i^{th}$  dc source (if all the dc sources have the same value  $V_{dc}$ , then  $V_1 = V_2 = \dots = V_s = 1$ ). The objective here is to choose the switching angles  $0 \leq \theta_1 < \theta_2 < \dots < \theta_s \leq \pi/2$  so as to make the first harmonic equal to the desired fundamental voltage  $V_f$  and specific higher harmonics of  $V(\omega t)$  equal to zero. As the application of interest here is a three-phase power system, the triplen harmonics in each phase need not be eliminated as they automatically cancel in the line-to-line voltages.

As an example, a three dc source case is now considered so that the switching angles are chosen so as to not generate the fifth- and seventh-order harmonics while achieving the desired fundamental voltage. The mathematical statement of these conditions is then

$$\begin{aligned} \frac{4V_{dc}}{\pi} (V_1 \cos(\theta_1) + V_2 \cos(\theta_2) + V_3 \cos(\theta_3)) &= V_f \\ V_1 \cos(5\theta_1) + V_2 \cos(5\theta_2) + V_3 \cos(5\theta_3) &= 0 \\ V_1 \cos(7\theta_1) + V_2 \cos(7\theta_2) + V_3 \cos(7\theta_3) &= 0. \end{aligned} \quad (2)$$

This is a system of three transcendental equations in the unknowns  $\theta_1$ ,  $\theta_2$ , and  $\theta_3$ . One approach to solving this set of non-linear transcendental equations (2) is to use an iterative method such as the Newton-Raphson method [11]. In this work, the method given in [12] is extended to find *all* solutions to (2). This methodology is based on the mathematical theory of resultants of polynomials which is a systematic procedure for finding the roots of systems of *polynomial* equations [13]. To use the method, the set of equations (2) is first converted to a polynomial system by setting  $x_1 = \cos(\theta_1)$ ,  $x_2 = \cos(\theta_2)$ ,  $x_3 = \cos(\theta_3)$ , and using the trigonometric identities  $\cos(5\theta) = 5\cos(\theta) - 20\cos^3(\theta) + 16\cos^5(\theta)$ ,  $\cos(7\theta) = -7\cos(\theta) + 56\cos^3(\theta) - 112\cos^5(\theta) + 64\cos^7(\theta)$  to transform (2) into the equivalent conditions

$$\begin{aligned} p_1(x) &\triangleq V_1 x_1 + V_2 x_2 + V_3 x_3 - m = 0 \\ p_5(x) &\triangleq \sum_{i=1}^3 V_i (5x_i - 20x_i^3 + 16x_i^5) = 0 \\ p_7(x) &\triangleq \sum_{i=1}^3 V_i (-7x_i + 56x_i^3 - 112x_i^5 + 64x_i^7) = 0 \end{aligned} \quad (3)$$

where  $x = (x_1, x_2, x_3)$  and  $m \triangleq V_f / (4V_{dc}/\pi)$ . The modulation index is  $m_a = m/s = V_f / (s4V_{dc}/\pi)$ . This follows from the fact that each inverter has a dc source that is nominally equal to  $V_{dc}$  so that the maximum output voltage of the multilevel inverter is  $sV_{dc}$ . Consequently, a square wave of amplitude  $sV_{dc}$  results in the maximum fundamental output possible of  $V_{f_{max}} = 4sV_{dc}/\pi$  so that  $m_a \triangleq V_f / V_{f_{max}} = V_f / (s4V_{dc}/\pi) = m/s$ .

This is now a set of three *polynomial* equations in the three unknowns  $x_1, x_2, x_3$  (see also [14] where a polynomial system was used). Further, the solutions must satisfy  $0 \leq x_3 < x_2 < x_1 \leq 1$ .

Next, one substitutes  $x_3 = (m - (V_1x_1 + V_2x_2))/V_3$  into  $p_5$ ,  $p_7$  to get

$$\begin{aligned} p_5(x_1, x_2) = & V_1(5x_1 - 20x_1^3 + 16x_1^5) + V_2(5x_2 - 20x_2^3 + 16x_2^5) \\ & + 5V_3 \left( \frac{m - (V_1x_1 + V_2x_2)}{V_3} \right) \\ & - 20V_3 \left( \frac{m - (V_1x_1 + V_2x_2)}{V_3} \right)^3 \\ & + 16V_3 \left( \frac{m - (V_1x_1 + V_2x_2)}{V_3} \right)^5 \end{aligned}$$

and

$$\begin{aligned} p_7(x_1, x_2) = & V_1(-7x_1 + 56x_1^3 - 112x_1^5 + 64x_1^7) \\ & + V_2(-7x_2 + 56x_2^3 - 112x_2^5 + 64x_2^7) \\ & - 7V_3 \left( \frac{m - (V_1x_1 + V_2x_2)}{V_3} \right) \\ & + 56V_3 \left( \frac{m - (V_1x_1 + V_2x_2)}{V_3} \right)^3 \\ & - 112V_3 \left( \frac{m - (V_1x_1 + V_2x_2)}{V_3} \right)^5 \\ & + 64V_3 \left( \frac{m - (V_1x_1 + V_2x_2)}{V_3} \right)^7. \end{aligned}$$

### A. Elimination Using Resultants

In order to explain how one computes the zero sets of polynomial systems, a brief discussion of the procedure of solving such systems is now given. A systematic procedure to do this is known as *elimination theory* and uses the notion of *resultants* [15], [16]. Briefly, one considers  $a(x_1, x_2)$  and  $b(x_1, x_2)$  as polynomials in  $x_2$  whose coefficients are polynomials in  $x_1$ . Then, for example, letting  $a(x_1, x_2)$  and  $b(x_1, x_2)$  have degrees 3 and 2, respectively in  $x_2$ , they may be written in the form

$$\begin{aligned} a(x_1, x_2) &= a_3(x_1)x_2^3 + a_2(x_1)x_2^2 + a_1(x_1)x_2 + a_0(x_1) \\ b(x_1, x_2) &= b_2(x_1)x_2^2 + b_1(x_1)x_2 + b_0(x_1). \end{aligned}$$

The  $n \times n$  *Sylvester* matrix, where  $n = \deg_{x_2}\{a(x_1, x_2)\} + \deg_{x_2}\{b(x_1, x_2)\} = 3 + 2 = 5$ , is defined by

$$S_{a,b}(x_1) = \begin{bmatrix} a_0(x_1) & 0 & b_0(x_1) & 0 & 0 \\ a_1(x_1) & a_0(x_1) & b_1(x_1) & b_0(x_1) & 0 \\ a_2(x_1) & a_1(x_1) & b_2(x_1) & b_1(x_1) & b_0(x_1) \\ a_3(x_1) & a_2(x_1) & 0 & b_2(x_1) & b_1(x_1) \\ 0 & a_3(x_1) & 0 & 0 & b_2(x_1) \end{bmatrix}.$$

The *resultant* polynomial is then defined by

$$r(x_1) = \text{Res}(a(x_1, x_2), b(x_1, x_2), x_2) \triangleq \det S_{a,b}(x_1) \quad (4)$$

and is the result of solving  $a(x_1, x_2) = 0$  and  $b(x_1, x_2) = 0$  simultaneously for  $x_1$ , i.e., eliminating  $x_2$ . See [13], [15]–[17] for an explanation of this fact. The computational challenge for this approach is in the symbolic calculation of the determinant of the Sylvester matrix. However, the results in [18], [19] show that this computation can be carried out quite efficiently.

### B. Switching Angle Solutions

The goal here is to find simultaneous solutions of  $p_5(x_1, x_2) = 0$ ,  $p_7(x_1, x_2) = 0$ . For each fixed  $x_1$ ,  $p_5(x_1, x_2)$  can be viewed as a polynomial in  $x_2$  whose coefficients are polynomials in  $x_1$ . For each fixed  $x_1$ , the pair of polynomials  $p_5(x_1, x_2) = 0$ ,  $p_7(x_1, x_2) = 0$  has a solution  $x_2$  if and only if their corresponding *resultant matrix*  $S_{p_5, p_7}(x_1)$  is singular. Here,  $\deg_{x_2}\{p_5(x_1, x_2)\} = 5$  and  $\deg_{x_2}\{p_7(x_1, x_2)\} = 7$  so that the resultant matrix  $S_{p_5, p_7}(x_1)$  is an element of  $\mathbb{R}^{12 \times 12}[x_1]$  and its determinant  $r_{5,7}(x_1) \triangleq \det S_{p_5, p_7}(x_1)$  is a *polynomial* in  $x_1$ .

The key point here is that for any  $(x_1, x_2)$  which is a simultaneous solution of  $p_5(x_1, x_2) = 0$ ,  $p_7(x_1, x_2) = 0$ , it must be that  $r_{5,7}(x_1) = 0$ . Consequently, finding the roots of  $r_{5,7}(x_1) = 0$  gives candidate values for  $x_1$  to check for common zeros of  $p_5(x_1, x_2) = 0$ ,  $p_7(x_1, x_2) = 0$ . The resultant polynomial  $r_{5,7}(x_1)$  of the pair  $\{p_5(x_1, x_2), p_7(x_1, x_2)\}$  was found with MATHEMATICA using the `Resultant` command and turned out to be a 35th-order polynomial. The explicit algorithm implemented to compute the switching angles is as follows.

#### Algorithm for the Seven-Level Case

- 1) Given  $m$  and the measured values of  $V_1, V_2, V_3$ , find the roots of  $r_{5,7}(x_1) = 0$ .
- 2) Discard any roots that are less than zero, greater than 1 or that are complex. Denote the remaining roots as  $\{x_{1i}\}$ .
- 3) For each fixed zero  $x_{1i}$  in the set  $\{x_{1i}\}$ , substitute it into  $p_5$  and solve for the roots of  $p_5(x_{1i}, x_2) = 0$ .
- 4) Discard any roots (in  $x_2$ ) that are complex, less than zero or greater than one. Denote the pairs of remaining roots as  $\{(x_{1j}, x_{2j})\}$ .
- 5) Compute  $m - (V_1x_{1j} + V_2x_{2j})/V_3$  and discard any pair  $(x_{1j}, x_{2j})$  that makes this quantity negative or greater than one. Denote the triples of remaining roots as  $\{(x_{1k}, x_{2k}, x_{3k})\}$ .
- 6) Discard any triple for which  $x_{3k} < x_{2k} < x_{1k}$  does not hold. Denote the remaining triples as  $\{(x_{1l}, x_{2l}, x_{3l})\}$ .

The switching angles that are a solution to the three-level system (2) are

$$\{(\theta_{1l}, \theta_{2l}, \theta_{3l})\} = \{(\cos^{-1}(x_{1l}), \cos^{-1}(x_{2l}), \cos^{-1}(x_{3l}))\}.$$

This algorithm was used to find the switching angles for each phase in a multilevel inverter with nonequal dc sources. The results for phase  $a$  are plotted in Fig. 3 where dc source voltages for this phase were measured to be  $V_1V_{dc} = 60.0$  V,  $V_2V_{dc} = 47.0$  V and  $V_3V_{dc} = 43.1$  V. It is important to note that the interest here is in a *symbolic* expression for the final resultant polynomial. That is, the final resultant polynomial is more precisely written as  $r(x_1, m, V_{dc1}, V_{dc2}, V_{dc3})$  showing that not only is it a function of the indeterminate  $x_1$ , but also of the parameters  $m, V_{dc1}, V_{dc2}, V_{dc3}$ . This is the desired form because, for example, in a hybrid electric vehicle the batteries powering the vehicle will not usually be at the same voltage level and will vary with use. Consequently, the dc source voltages could be measured, and the switching angles in Fig. 3 could be recomputed *online* to account for changes in the source voltages. This is because, starting with  $r(x_1, m, V_{dc1}, V_{dc2}, V_{dc3})$ ,

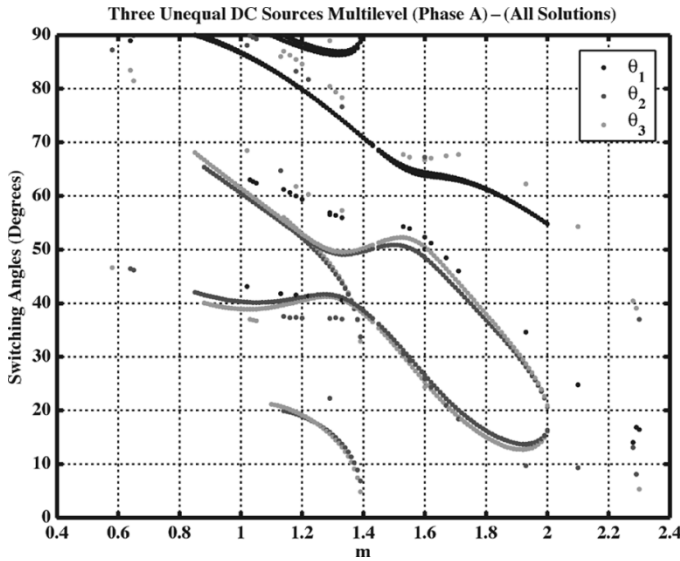


Fig. 3. All solution sets  $\{\theta_1, \theta_2, \theta_3\}$  versus  $m$ .

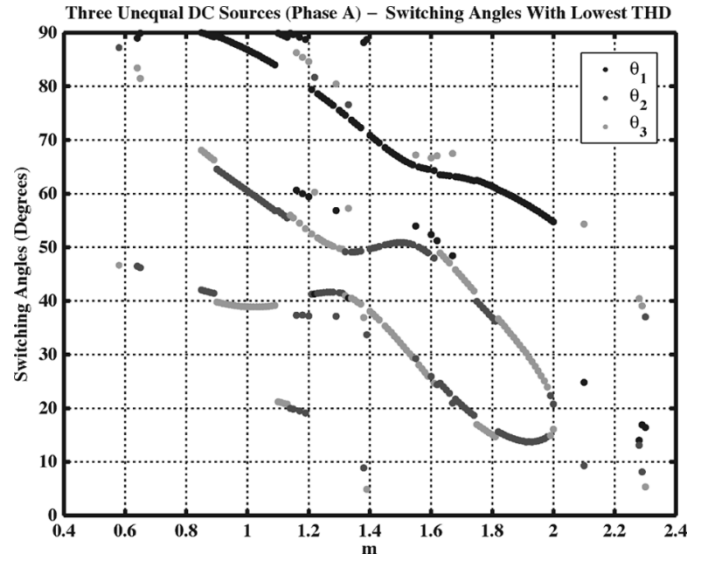


Fig. 5. The solution set  $\{\theta_1, \theta_2, \theta_3\}$  versus  $m$  that gives the smallest possible THD.

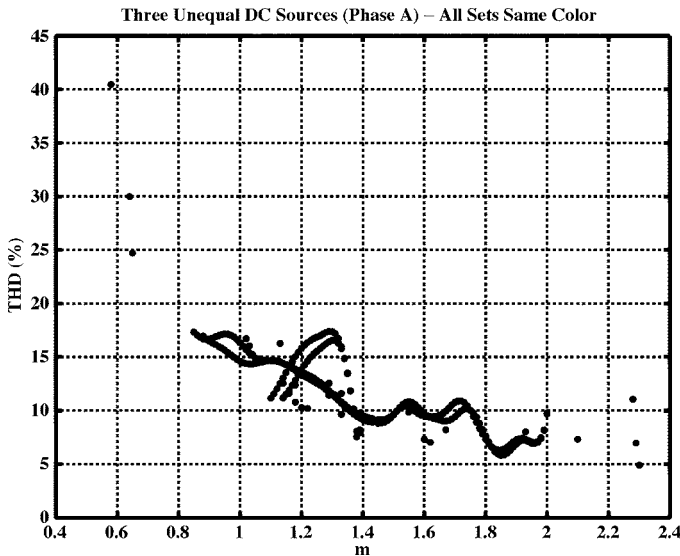


Fig. 4. Total harmonic distortion versus  $m$  for all possible switching angles solutions.

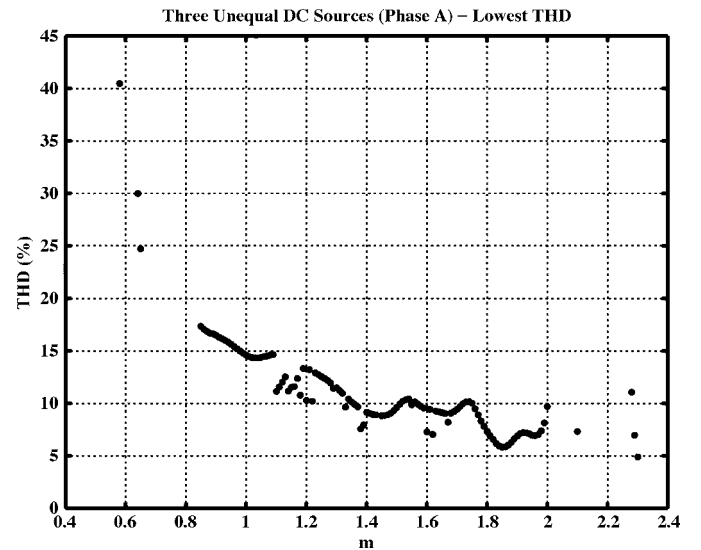


Fig. 6. Total harmonic distortion versus  $m$  for the switching angles that result in the smallest THD.

the calculation to compute the data of Fig. 3 takes less than a second for any given modulation index. In contrast, if iterative numerical techniques are used, one is not guaranteed that the solution will converge (the initial guess has to be “close” to the solution or there may be no solution), nor that the particular solution obtained is the only solution and, therefore, the best in any sense.

Fig. 3 shows the switching angles  $\theta_1, \theta_2, \theta_3$  versus  $m$  for those values of  $m$  in which the system (2) has at least one solution set. The parameter  $m$  was incremented in steps of 0.01. Note that for  $m$  in the range from approximately 1.1 to 2.0, there are at least two different sets of solutions and sometimes three sets.

One clear way to choose a particular solution is simply to pick the one that results in the smallest THD. This is shown in Fig. 4 corresponding to the solutions given in Fig. 3. Choosing the switching angles based on this criteria, the multiple switching

angle solutions given in Fig. 3 reduce to the single set of solutions given in Fig. 5, and the corresponding THD is shown in Fig. 6.

#### IV. EXPERIMENTAL WORK

A prototype three-phase 11-level wye-connected cascaded inverter has been built using 100-V 70-A MOSFETs as the switching devices. The gate driver boards and MOSFETs are shown in Fig. 7. A battery bank of 15 SDCSs of 60 V dc (nominally) each feed the inverter configured with five SDCSs per phase [20]. In the experimental study here, this prototype system was configured to be seven levels (three SDCSs per phase).

The ribbon cable shown in the figure provides the communication link between the gate driver board and the real-time processor. In this work, a real-time computing platform [21] was

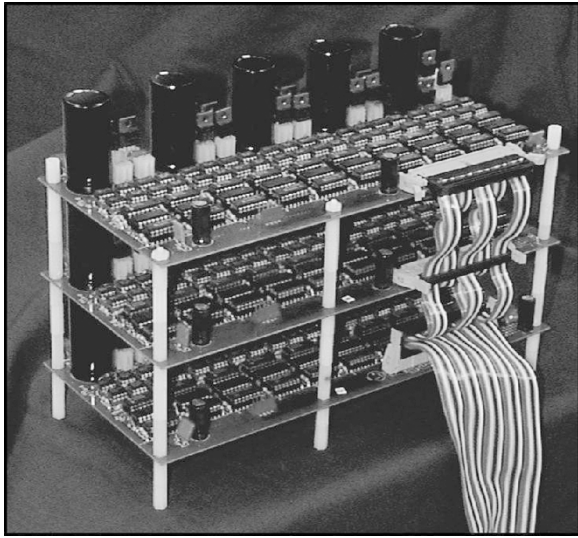


Fig. 7. Gate driver boards and MOSFETs for the multilevel inverter.

TABLE I  
EXPERIMENTAL H-BRIDGE DC-LINK VOLTAGES

Phase	$V_1V_{dc}$	$V_2V_{dc}$	$V_3V_{dc}$
<i>a</i>	60.0 V	47.0 V	43.1 V
<i>b</i>	59.9 V	48.4 V	43.1 V
<i>c</i>	60.1 V	47.3 V	41.4 V

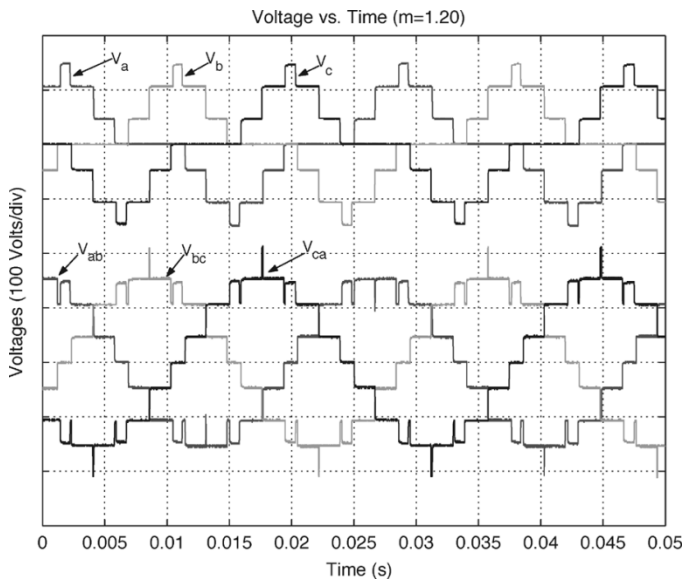


Fig. 8. Three-phase voltage waveforms for  $m_a = 0.4$  ( $m = 1.2$ ).

used to interface the computer (which generates the logic signals) to this cable. This system allows one to implement the switching algorithm as a lookup table in SIMULINK which is then converted to *C* code using RTW (real-time workshop) from The MathWorks Inc. The software provides icons to interface the SIMULINK model to the digital I/O board and converts the *C* code into executables.

The time resolution (the precision for the time at which a switch is turned on or off) was chosen to be 1/1000 of an electrical cycle. For a 60-Hz frequency requirement, this comes to

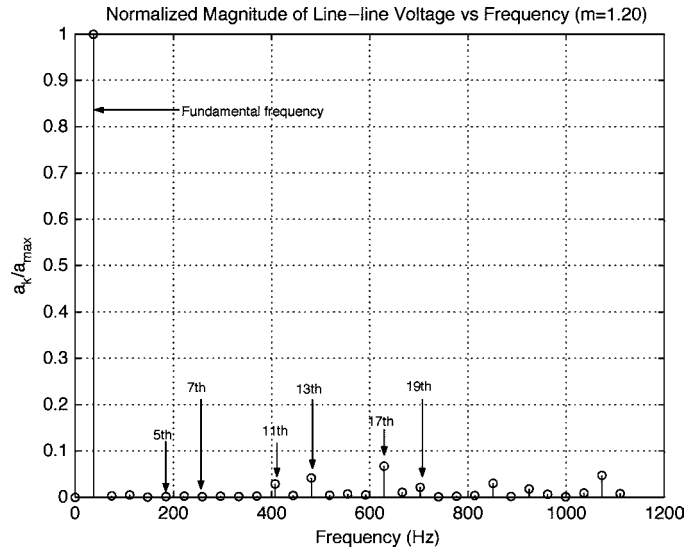


Fig. 9. Fast Fourier transform (FFT) of the line-line voltage between phases *a* and *b*.

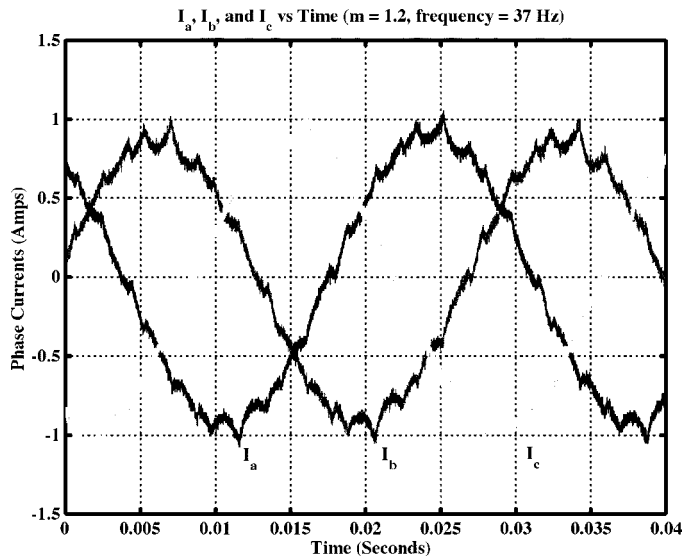


Fig. 10. Phase currents versus time in seconds for  $m_a = 0.4$  ( $m = 1.2$ ).

$(1/60)/1000 = 16.7 \mu s$ . Note that while the computation of the lookup table of Fig. 5 requires some offline computational effort, the real-time implementation is accomplished by putting the data (i.e., Fig. 5) in a lookup table and, therefore, does not require high computational power for implementation.

The multilevel converter was attached to a three-phase induction motor with the following nameplate data:

- rated horsepower = 1/3 hp
- rated current = 1.5 A
- rated speed = 1725 r/min
- rated voltage = 208 V (rms line-to-line at 60 Hz).

The voltage for each separate dc source of each phase was measured and is given in Table I. In the first set of experiments, the parameter  $m$  was set equal to 1.2 (for a modulation index  $m_a = 1.2/3 = 0.4$ ), and the frequency was set to 60 Hz.

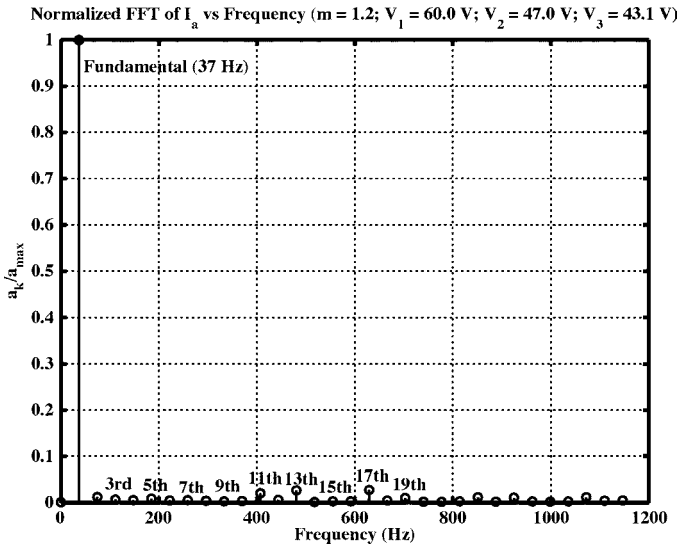


Fig. 11. Normalized FFT of the phase  $a$  current shown in Fig. 10.

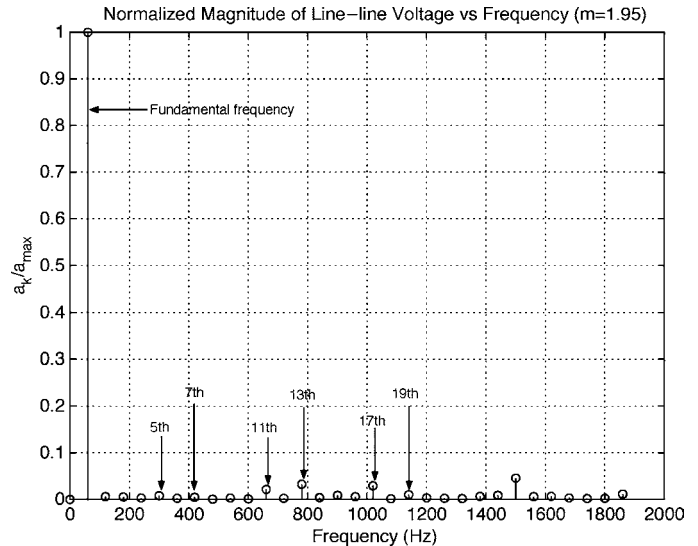


Fig. 13. Normalized FFT of the line-line voltage between phases  $a$  and  $b$ .

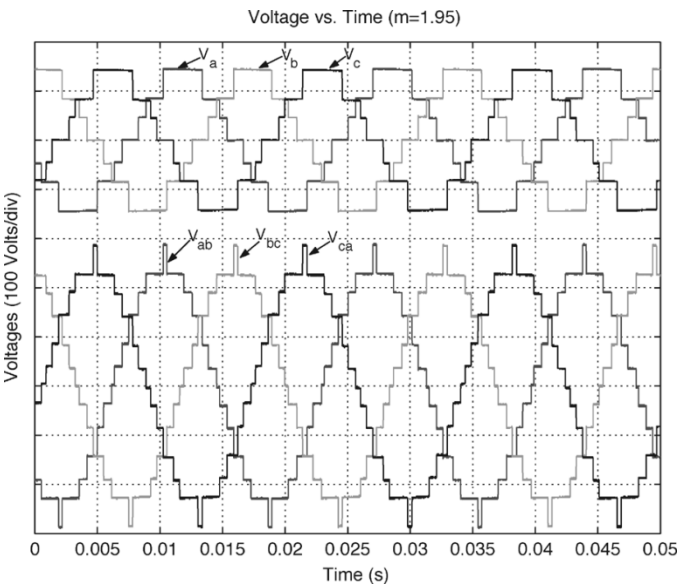


Fig. 12. Voltage waveforms for  $m_a = 0.65$  ( $m = 1.95$ ).

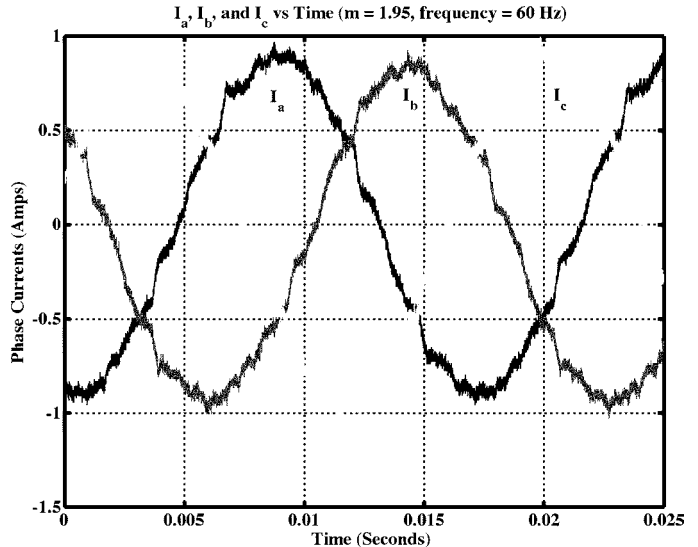


Fig. 14. Current waveforms for  $m_a = 0.65$  ( $m = 1.95$ ).

The switching angles for phase  $a$  were taken from Fig. 5 with  $m = 1.2$  while a similar computation was done to obtain the switching angles for phases  $b$  and  $c$ . The resulting three phase voltages were measured, and both the phase and line-line voltages are shown in Fig. 8. The FFT of the line-line voltage between phases  $a$  and  $b$  is shown in Fig. 9.

Note that the fifth and seventh harmonics are zero as predicted. The phase currents in the motor produced by the voltages of Fig. 8 are shown in Fig. 10. The FFT of the current waveform of phase  $a$  is shown in Fig. 11. Note that the harmonic content of the current is significantly reduced compared to the harmonic content of the voltage due to filtering by the motor's inductance. The THD for the current waveform of phase  $a$  was computed from the FFT of Fig. 11 and found to be 4.8%.

In the second set of experiments, the parameter  $m$  was set equal to 1.95 (for a modulation index  $m_a = 1.95/3 = 0.65$ ), and the frequency was set to 60 Hz. The switching angles for phase  $a$  were again taken from Fig. 5 with  $m = 1.95$  while a similar computation was done to obtain the switching angles for phases  $b$  and  $c$ . Both the phase and line-line voltages applied to the motor are shown in Fig. 12, and the FFT of the line-line voltage between phases  $a$  and  $b$  is given in Fig. 13. Note that the fifth and seventh harmonics are zero as predicted.

Fig. 14 shows the three-phase motor currents resulting from applying the voltages of Fig. 12 to the motor. The FFT of the current waveform of phase  $a$  is shown in Fig. 15. Again, the harmonic content of the current is significantly reduced compared to the harmonic content of the voltage because of filtering by the motor's inductance. The THD for the current waveform of phase  $a$  was computed using the FFT data of Fig. 15 and was found to be 4.15%.

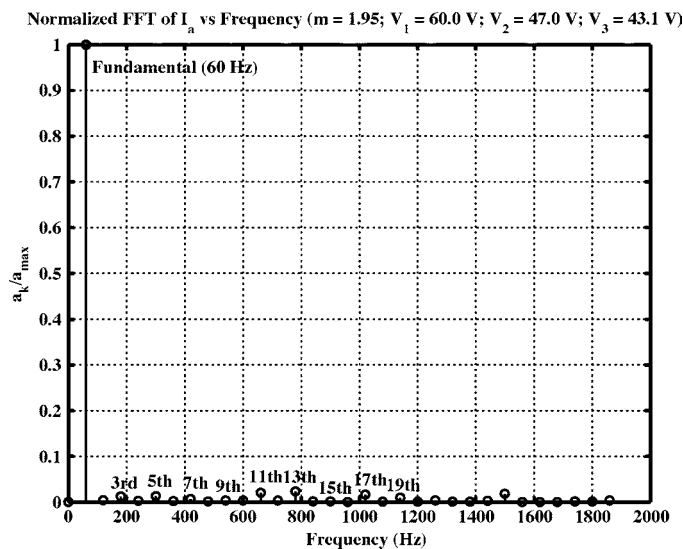


Fig. 15. FFT of the phase-*a* current waveform shown in Fig. 14.

## V. CONCLUSION

Elimination theory and the notion of resultants can be used to eliminate the lower order harmonics in a multilevel converter that has nonequal dc sources. This method is expected to have widespread application as most multilevel converters do not have dc sources that are exactly equal.

## ACKNOWLEDGMENT

The authors would like to thank Oak Ridge National Laboratory for providing the multilevel converter used in the experiments.

## REFERENCES

- [1] J. Chiasson, L. M. Tolbert, K. McKenzie, and Z. Du, "A complete solution to the harmonic elimination problem," *IEEE Trans. Power Electron.*, vol. 19, no. 2, pp. 491–499, Mar. 2004.
- [2] —, "Control of a multilevel converter using resultant theory," *IEEE Trans. Contr. Syst. Technol.*, vol. 11, no. 3, pp. 345–354, May 2003.
- [3] Z. Jiang and T. A. Lipo, "Switching angles and dc link voltage optimization for multilevel cascade inverters," *Elect. Mach. Power Syst.*, vol. 28, pp. 605–612, Jul. 2000.
- [4] Z. Du, L. M. Tolbert, and J. N. Chiasson, "Active harmonic elimination in multilevel converters using FPGA control," in *Proc. 9th IEEE Workshop Computers in Power Electronics, COMPEL'04*, Aug. 2004, CD-ROM.
- [5] B. Özpıneci, L. M. Tolbert, and J. N. Chiasson, "Harmonic optimization of multilevel converters using genetic algorithms," in *Proc. IEEE PESC'04*, Aachen, Germany, Jun. 2004, pp. 3911–3916.
- [6] P. N. Enjeti, P. D. Ziogas, and J. F. Lindsay, "Programmed PWM techniques to eliminate harmonics: a critical evaluation," *IEEE Trans. Ind. Appl.*, vol. 26, no. 2, pp. 302–316, Mar./Apr. 1990.
- [7] R. Lund, M. D. Manjrekar, P. Steimer, and T. A. Lipo, "Control strategies for a hybrid seven-level inverter," in *Proc. Eur. Power Electronics Conf.*, Lausanne, Switzerland, Sep. 1999, CD-ROM.
- [8] M. Manjrekar and T. Lipo, "A hybrid multilevel inverter topology for drive applications," in *Proc. IEEE APEC'98*, Anaheim, CA, Feb. 1998, pp. 523–529.
- [9] D. G. Holmes and B. P. McGrath, "Opportunities for harmonic cancellation with carrier-based pwm for two-level and multilevel cascaded inverters," *IEEE Trans. Ind. Appl.*, vol. 37, no. 2, pp. 574–582, Mar./Apr. 2001.

- [10] J. S. Lai and F. Z. Peng, "Multilevel converters—a new breed of power converters," *IEEE Trans. Ind. Appl.*, vol. 32, no. 3, pp. 509–517, May/Jun. 1996.
- [11] T. Cunningham, "Cascade multilevel inverters for large hybrid-electric vehicle applications with variant DC sources," Master's thesis, Dept. Elect. Comput. Eng., Univ. Tennessee, Knoxville, 2001.
- [12] J. Chiasson, L. M. Tolbert, K. McKenzie, and Z. Du, "Eliminating harmonics in a multilevel inverter using resultant theory," in *Proc. IEEE PESC'02*, Cairns, Australia, Jun. 2002, pp. 503–508.
- [13] T. Kailath, *Linear Systems*. Englewood Cliffs, NJ: Prentice-Hall, 1980.
- [14] J. Sun and I. Grotstollen, "Pulsewidth modulation based on real-time solution of algebraic harmonic elimination equations," in *Proc. IEEE IECON'94*, vol. 1, 1994, pp. 79–84.
- [15] D. Cox, J. Little, and D. O'Shea, *Ideals, Varieties, and Algorithms: An Introduction to Computational Algebraic Geometry and Commutative Algebra*, 2nd ed. Berlin, Germany: Springer-Verlag, 1996.
- [16] J. von zur Gathen and J. Gerhard, *Modern Computer Algebra*. Cambridge, U.K.: Cambridge Univ. Press, 1999.
- [17] C. Chen, *Linear Systems Theory and Design*, 3rd ed. London, U.K.: Oxford Univ. Press, 1999.
- [18] M. Hromcik and M. Sebek, "New algorithm for polynomial matrix determinant based on FFT," in *Proc. Eur. Conf. Control, ECC'99*, Karlsruhe, Germany, Aug. 1999, CD-ROM.
- [19] —, "Numerical and symbolic computation of polynomial matrix determinant," in *Proc. Conf. Decision and Control*, Tampa, FL, 1999, pp. 1887–1888.
- [20] L. M. Tolbert, F. Z. Peng, T. Cunningham, and J. Chiasson, "Charge balance control schemes for cascade multilevel converter in hybrid electric vehicles," *IEEE Trans. Ind. Electron.*, vol. 49, no. 5, pp. 1058–1064, Oct. 2002.
- [21] Opal-RT Technologies. (2001) RTLab. [Online]. Available: <http://www.opal-rt.com/>



**Leon M. Tolbert** (S'89–M'91–SM'98) received the B.E.E., M.S., and Ph.D. degrees in electrical engineering from the Georgia Institute of Technology, Atlanta.

He joined the Engineering Division of Lockheed Martin Energy Systems in 1991 and worked on several electrical distribution projects at the three U.S. Department of Energy plants in Oak Ridge, TN. In 1997, he became a Research Engineer in the Power Electronics and Electric Machinery Research Center, Oak Ridge National Laboratory. In 1999, he was appointed as an Assistant Professor in the Department of Electrical and Computer Engineering, The University of Tennessee, Knoxville. He is an adjunct participant at Oak Ridge National Laboratory and conducts joint research at the National Transportation Research Center (NTRC). He does research in the areas of electric power conversion for distributed energy sources, motor drives, multilevel converters, hybrid electric vehicles, and application of SiC power electronics.

Dr. Tolbert is a Registered Professional Engineer in the State of Tennessee. He is the recipient of a National Science Foundation CAREER Award and the 2001 IEEE Industry Applications Society Outstanding Young Member Award. He is an Associate Editor of the IEEE POWER ELECTRONICS LETTERS.

He is an Associate Editor of the IEEE POWER ELECTRONICS LETTERS.



**John N. Chiasson** (S'82–M'84–SM'03) received the Bachelor's degree in mathematics from the University of Arizona, Tucson, the Master's degree in electrical engineering from Washington State University, Pullman, and the Ph.D. degree in controls from the University of Minnesota, Minneapolis.

He has worked in industry at Boeing Aerospace, Control Data, and ABB Daimler-Benz Transportation. Since 1999, has been with the Department of Electrical and Computer Engineering, The University of Tennessee, Knoxville, where his current interests

include the control of ac drives, nonlinear system identification, and multilevel converters.



**Zhong Du** (S'01) received the B.S. and M.S. degrees from Tsinghua University, Beijing, China, in 1996 and 1999, respectively. He is currently working toward the Ph.D. degree in electrical and computer engineering at The University of Tennessee, Knoxville.

He has worked in the area of computer networks, both in academia as well as in industry. His research interests include power electronics and computer networks.



**Keith J. McKenzie** (S'01) received the B.S. and M.S. degrees in electrical engineering from The University of Tennessee, Knoxville, in 2001 and 2004, respectively. He is currently working toward the Ph.D. degree in The Bradley Department of Electrical and Computer Engineering, Virginia Polytechnic Institute and State University, Blacksburg.